

Expansion of harmonically trapped interacting particles and time dependence of the contact

Chunlei Qu^{1,*}, Lev P. Pitaevskii^{1,2}, and Sandro Stringari¹

¹*INO-CNR BEC Center and Dipartimento di Fisica, Università di Trento, 38123 Povo, Italy*

²*Kapitza Institute for Physical Problems RAS, Kosygina 2, 119334 Moscow, Russia*

(Dated: March 28, 2022)

We study the expansion of an interacting atomic system at zero temperature, following its release from an isotropic three-dimensional harmonic trap and calculate the time dependence of its density and momentum distribution, with special focus on the behavior of the contact parameter. We consider different quantum system, including the unitary Fermi gas of infinite scattering length, the weakly interacting Bose gas and two interacting particles with highly asymmetric mass imbalance. In all cases analytic results can be obtained, which show that the initial value of the contact, fixing the $1/k^4$ tail of the momentum distribution, disappears for large expansion times. Our results raise the problem of understanding the recent experiment of R. Chang *et al.* (arXiv:1608.04693) carried out on a weakly interacting Bose gas of metastable ^4He atoms, where a $1/r^4$ tail in the density distribution was observed after a large expansion time, implying the existence of the $1/k^4$ tail in the asymptotic momentum distribution.

I. INTRODUCTION

It is well known that the momentum distribution $n(k)$ of a system of interacting particles exhibits, at equilibrium, the scaling behavior \mathcal{C}/k^4 at large momenta k , where the coefficient \mathcal{C} defines the total Tan contact [1], a universal quantity connecting the thermodynamic properties of the many-body system to the short range behavior of its wave function [1–7]. In the case of a weakly interacting Bose gas this tail is physically associated with the presence of the quantum depletion of the condensate, a challenging feature well understood theoretically, but difficult to measure experimentally [8–10]. The $1/k^4$ tail of the momentum distribution has been measured in the unitary Fermi gas, profiting of the possibility of turning off the interaction, just after the release of the trap [11, 12]. In this case the momentum distribution is conserved during the expansion, so that experiments measure the value of the contact before expansion. Despite the systematic investigations of the contact at equilibrium [13–21], its evolution in a dynamical context has been rarely explored [22–25]. The importance of this question is manifested by the fact that the momentum distribution is affected by interactions during the expansion and, for large expansion times, when it becomes time-independent, can be directly related to the measurable time-dependent density distribution $\rho(\mathbf{r}, t)$ through the ballistic relationship

$$n_{\text{asym}}(\mathbf{k}) = \lim_{t \rightarrow \infty} (\hbar t/m)^3 \rho(\mathbf{r} = \hbar \mathbf{k} t/m, t). \quad (1)$$

According to Eq.(1), an asymptotic $1/k^4$ tail in the momentum distribution should show up in a tail of the density distribution, characterized by the t/r^4 dependence for large values of r and t . A recent experiment [26],

where the density distribution of an expanding gas of metastable ^4He atoms was measured with high accuracy, has indicated that the contact parameter \mathcal{C} is actually increased with respect to the initial value, and thus motivated us for the theoretical investigation of the dynamical evolution of the contact.

The mechanism of the expansion of a dilute atomic gas is well understood in the regime of distances satisfying the condition $r \leq R_{\text{TF}}(t)$, where $R_{\text{TF}}(t)$ is the Thomas-Fermi radius at the expansion time t , or momenta smaller than the inverse of the healing length [27]. In this regime approximate schemes based on scaling transformations [28, 29] or on the hydrodynamic picture [30] provide an accurate description of the expansion and, in particular, have proven very successful in predicting the time dependence of the aspect ratio, a quantity measurable with high precision.

The description of the expansion at a more microscopic level, involving the large- k components of the momentum distribution, represents a more challenging problem, whose solution requires the implementation of time-dependent dynamic theories beyond the mean field level. The purpose of the present work is to discuss some examples where such theories can be worked out explicitly and the question of the behavior of the tails of the momentum distribution can be addressed in a quantitative way at zero temperature. These include the unitary Fermi gas, the weakly interacting Bose gas and the two-body problem with highly asymmetric mass imbalance which reduces the problem to the solution of the single-particle Schrödinger equation.

The paper is structured as follows. In Sec. II we investigate the evolution of the contact for the unitary Fermi gas and the weakly repulsive Bose gas. In Sec. III we explicitly calculate the density and momentum distributions during the expansion for the two-particle system, both at unitarity and in the case of weakly repulsive interaction. In both cases the contact is found to decrease for large expansion times in the same way as in the cor-

* chunleiqu@gmail.com

responding many-body systems. We also calculate the change of the contact after a sudden quench of the scattering length from a small value to infinity just before the expansion. Our concluding remarks are reported in Sec. IV.

II. MANY-BODY INTERACTING SYSTEMS

A. Unitary Fermi gas

A remarkable feature exhibited by the Fermi gas at unitarity is that an exact solution of the problem of the expansion from a three-dimensional (3D) isotropic harmonic trap can be formulated in terms of the exact scaling transformation [31]

$$\psi(\mathbf{r}_1, \dots, \mathbf{r}_N, t) = \mathcal{N}(t) e^{i \sum_j \frac{m r_j^2}{2\hbar} \frac{\dot{b}}{b}} \psi_0\left(\frac{\mathbf{r}_1}{b}, \dots, \frac{\mathbf{r}_N}{b}\right) \quad (2)$$

of the many-body wave-function. Here N is the number of particles, $|\mathcal{N}(t)| = b^{-3N/2}$ is the normalization constant and $b(\tau) = \sqrt{1 + \tau^2}$ with $\tau = \omega_{\text{ho}} t$ the dimensionless time and ω_{ho} the trapping frequency.

Consequently, the density distribution of the system during the expansion, is given by

$$\rho(r, \tau) = \frac{1}{(1 + \tau^2)^{3/2}} \rho_0(r/\sqrt{1 + \tau^2}), \quad (3)$$

where $\rho_0(r)$ is the equilibrium density evaluated at $t = 0$. The ballistic relation (Eq. (1)) then gives the following expression for the asymptotic momentum distribution

$$n_{\text{asym}}(k) = (\hbar/m\omega_{\text{ho}})^3 \rho_0(r = \hbar k/m\omega_{\text{ho}}), \quad (4)$$

which holds for large times satisfying the condition $t \gg 1/\omega_{\text{ho}}$. The scaling result shows that the occurrence of the $1/k^4$ tail in $n_{\text{asym}}(k)$ should be associated with a corresponding $1/r^4$ tail at large r in the equilibrium density distribution before expansion. This behavior is ruled out by the simple argument that no natural cut-off exists in coordinate space at large r and that the $1/r^4$ law would imply an unphysical infrared divergent behavior in the ground state harmonic oscillator energy.

An explicit expression for the time dependence of the contact can be obtained by making the adiabatic ansatz [1]. This ansatz corresponds to assuming that, during the expansion, the large momentum component of the momentum distribution is given by the same expression $\mathcal{C}(t)/k^4$ holding at equilibrium, with $\mathcal{C}(t)$ evaluated using the time dependent value of the density profile. The adiabatic ansatz holds if the two-body interaction, which dictates the short range behavior of the wave function, is kept constant or slowly varying in time. In the unitary Fermi gas the contact is given by $\mathcal{C}(t) = (2\pi)^{-3} \int d\mathbf{r} \{ \alpha [3\pi^2 \rho(\mathbf{r}, t)]^{4/3} \}$ where $\alpha \simeq 0.12$ is a universal parameter. Using the position and time dependence of the density predicted by the scaling law (Eq. (3)),

the contact is then expected to evolve in time as $\mathcal{C}(t) = \mathcal{C}_0/(1 + \omega_{\text{ho}}^2 t^2)^{1/2}$ where $\mathcal{C}_0 = 32\alpha N k_{\text{F}}^0 / (35\pi^2 \xi_{\text{B}}^{1/4})$ is the initial contact of the unitary Fermi gas at equilibrium, ξ_{B} is the Bertsch parameter, and $k_{\text{F}}^0 = [3\pi^2 \rho_0(0)]^{1/3}$ is the initial local Fermi momentum at the trap center.

It is worth noticing that the same analytic result (Eq. (4)) for the asymptotic momentum distribution and for the time dependence of the contact can be also derived by studying the behavior of the one-body density matrix (see Appendix A).

B. Weakly repulsive Bose gas

Although in the case of 3D Bose gas an exact scaling solution of the many-body wave function similar to Eq. (2) is not available, the adiabatic ansatz discussed above is still expected to hold, yielding the time dependence of the contact in the form $\mathcal{C}(t) = (2\pi)^{-3} \int d\mathbf{r} [16\pi^2 \rho^2(\mathbf{r}, t) a^2]$ where a is the s -wave scattering length and the integrand is the local contact density at equilibrium predicted by Bogoliubov theory. We can then use the time dependence of the density profile during the expansion as predicted by the use of scaling transformations or hydrodynamic theory to predict the decay of the contact as $\mathcal{C}(t) = \mathcal{C}_0/(1 + \omega_{\text{ho}}^2 t^2)^{3/2}$ where $\mathcal{C}_0 = 15N^2 a^2 / (7\pi^2 R_{\text{TF}}^3)$ is the initial contact of the dilute Bose gas with R_{TF} the initial Thomas-Fermi radius.

III. TWO-BODY PROBLEM

More complete and explicit results for the time evolution of the contact are available by solving the expansion dynamics of a two-body problem, which gives access to the exact time-dependence of the density and momentum distributions and provides explicit conditions for the applicability of the adiabaticity ansatz. For the sake of brevity, we consider two interacting particles in an isotropic 3D harmonic trap with one of them being so heavy that the center-of-mass motion can be ignored. This reduces the problem to the investigation of a one-body system described by the Hamiltonian

$$H = -\frac{\hbar^2}{2m} \nabla^2 + \frac{m}{2} \omega_{\text{ho}}^2 r^2 + V(r), \quad (5)$$

where m is the mass of the light particle. $V(r)$ is the two-body interaction characterized by the value of the s -wave scattering length, a quantity which, in the presence of a Fano-Feshbach resonance, can be tuned by applying an external magnetic field [32]. In this work, we will consider the regularized pseudopotential $V(r) = (2\pi\hbar^2 a/m) \delta^{(3)}(\mathbf{r}) \frac{\partial}{\partial r} r$, whose eigenvalue problem can be solved analytically [33]. The eigenfunctions take the form

$$\psi_0(r) = \frac{A}{\sqrt{\pi}} \frac{a}{a_{\text{ho}}^{5/2}} e^{-r^2/2a_{\text{ho}}^2} \Gamma(-\nu) U\left(-\nu, \frac{3}{2}, \frac{r^2}{a_{\text{ho}}^2}\right), \quad (6)$$

where $U(x, y, z)$ is the hypergeometric function, A is the normalization constant, $a_{\text{ho}} = \sqrt{\hbar/m\omega_{\text{ho}}}$ is the harmonic oscillator length and $\nu = (E/2\hbar\omega_{\text{ho}} - 3/4)$, with the eigenvalue E determined by

$$\frac{\Gamma(-E/2\hbar\omega_{\text{ho}} + 3/4)}{\Gamma(-E/2\hbar\omega_{\text{ho}} + 1/4)} = \frac{a_{\text{ho}}}{2a}. \quad (7)$$

Two different values of scattering length will be discussed in the following:

A. Unitary interaction

At unitarity ($a = \infty$), the ground state energy is $E = \hbar\omega_{\text{ho}}/2$ and the corresponding wave function takes the form $\psi_0(r) = \frac{1}{\sqrt{2\pi^{3/4}}a_{\text{ho}}^{-1/2}} \exp\left(-\frac{r^2}{2a_{\text{ho}}^2}\right)r^{-1}$. The wave function decays exponentially at large r whereas it approaches $1/r$ for small r . We notice that the size of the pair is reduced with respect to the non-interacting value according to $\langle r^2 \rangle_{\infty} / \langle r^2 \rangle_0 = 1/3$, reflecting the attractive nature of the force at unitarity.

The ground state wave function in momentum space is readily obtained after a Fourier transformation:

$$\phi_0(k) = \sqrt{\frac{2}{\pi}} \int_0^{\infty} \psi_0(r) \frac{\sin(kr)}{kr} r^2 dr = \frac{\sqrt{2}}{\pi^{5/4}} \frac{a_{\text{ho}}^{1/2}}{k} F\left(\frac{ka_{\text{ho}}}{\sqrt{2}}\right), \quad (8)$$

where $F(z) = e^{-z^2} \int_0^z e^{y^2} dy$ is the Dawson function. Using its asymptotic behavior [34], one finds the result

$$n_0(k) = \frac{2a_{\text{ho}}}{\pi^{5/2}k^2} \left[F\left(\frac{ka_{\text{ho}}}{\sqrt{2}}\right) \right]^2 = \begin{cases} \pi^{-5/2}a_{\text{ho}}^3, & k \rightarrow 0 \\ \frac{\pi^{-5/2}a_{\text{ho}}}{k^4}, & k \rightarrow \infty \end{cases} \quad (9)$$

for the momentum distribution, yielding the value $\mathcal{C}_0 = \pi^{-5/2}a_{\text{ho}}^{-1}$ for the contact.

When the particle is released from the isotropic trap, the wave function evolves according to the exact scaling transformation, Eq. (2) (with $N = 1$), thus the expanding density distribution is given by

$$\rho(r, \tau) = \frac{1}{2\pi^{3/2}(1 + \tau^2)^{1/2}} \exp\left[-\frac{r^2}{(1 + \tau^2)a_{\text{ho}}^2}\right] \frac{1}{r^2 a_{\text{ho}}}, \quad (10)$$

where $\tau = \omega_{\text{ho}}t$ is the dimensionless time. The density distribution exponentially decays at large r and the absence of an additional $1/r^4$ tail indicates that the $1/k^4$ tail of the momentum distribution will disappear at large expansion time. The time evolution of the momentum distribution can be explicitly obtained by calculating the wave function in momentum space. One finds

$$\phi(k, \tau) = \left(\frac{1 + i\tau}{1 - i\tau}\right)^{1/4} \frac{\sqrt{2}}{\pi^{5/4}} \frac{a_{\text{ho}}^{1/2}}{k} F\left(\sqrt{1 + i\tau} \frac{ka_{\text{ho}}}{\sqrt{2}}\right). \quad (11)$$

Therefore, as a consequence of the asymptotic behavior of the Dawson function [34], we find that, for any fixed

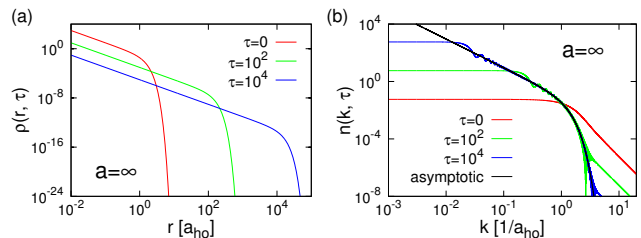


FIG. 1. (Color online) (a) The density distribution $\rho(r, \tau)$ and (b) momentum distribution $n(k, \tau)$ in the presence of a regularized pseudopotential with unitary interaction applied to the two-body problem. Different colors are the distributions at different expansion time $\tau = 0$ (red), 10^2 (green), 10^4 (blue) and the asymptotic momentum distribution (black). The linear part of the density distribution $\rho(r, \tau)$ at small r exhibits the $1/r^2$ behavior and the linear part of the momentum distribution $n(k, \tau)$ at large k exhibits the $1/k^4$ behavior for finite expansion times.

value of t , $n(k, t) = \mathcal{C}(t)/k^4$ for $ka_{\text{ho}} \rightarrow \infty$ with the contact $\mathcal{C}(t) = \mathcal{C}_0/\sqrt{1 + \omega_{\text{ho}}^2 t^2}$ vanishing like $1/t$ for large expansion times [35]. This is the same law obtained in the case of the unitary Fermi gas discussed in the first part of the paper, using the adiabaticity ansatz for the evolution of the contact.

The asymptotic momentum distribution, easily derivable by inserting Eq.(10) into the ballistic formula (Eq.(1)), takes the form

$$n_{\text{asym}}(k) = \frac{1}{2\pi^{3/2}} \frac{a_{\text{ho}}}{k^2} e^{-k^2 a_{\text{ho}}^2}. \quad (12)$$

The same expression for the asymptotic momentum distribution can be also obtained using the asymptotic $F(z) \rightarrow i\sqrt{\pi}e^{-z^2}/2$ of the Dawson function, holding for $|z| \rightarrow \infty$ and $\arg(z) \rightarrow \pi/4$. This result can be obtained using the relation between Dawson function and the error function $F(z) = i\sqrt{\pi}e^{-z^2} \text{erf}(-iz)/2$ and equation (7.2.4) from Ref. [36].

Figure 1 shows the density distribution $\rho(r, \tau)$ and the momentum distribution $n(k, \tau)$ at $\tau = 0, 10^2, 10^4$. The figure shows that the value of k , above which one can observe the $1/k^4$ behavior, becomes larger and larger as the increase of τ . We find that for $\tau = 10^4$ the $1/k^4$ tail is practically no longer visible and that the momentum distribution (see Fig. 1(b)), is indistinguishable from the asymptotic behavior, except for small values of k where reaching the asymptotic behavior requires even larger expansion times. It is also worth to note that, for shorter times, where the $1/k^4$ tail is still visible in the momentum distribution, there is no trace of the $1/r^4$ tail in the density distribution (see Fig. 1(a)) because the ballistic relationship (1) is not applicable on these times.

B. Weak repulsive interaction

In this case, the energy and the normalization constant must be determined numerically. Choosing $a = 0.05a_{\text{ho}}$, one finds $E \approx 1.557\hbar\omega_{\text{ho}}$ and $A \approx 0.43$ [37]. At small r , the exact wave function can be approximated by $\psi_0(r) \approx Aa_{\text{ho}}^{-3/2}(a/r - 1)$, whereas the large r behavior is dominated by the exponential factor. The momentum distribution at large k is determined by the small r behavior of the wave function. One finds the dependence $n_0(k) = 2\pi^{-1}A^2a_{\text{ho}}^{-3}a^2/k^4$ for large k , yielding the value $C_0 = 2\pi^{-1}A^2a_{\text{ho}}^{-3}a^2$ for the contact which is proportional to a^2 like the case of the weakly interacting Bose gas.

The problem of the expansion can be solved in a way similar to the one of Ref. [23], where the short time evolution of the contact was studied after quenching the scattering length to infinity in the presence of harmonic trap. After the release of the trap, the eigenfunctions of the continuous spectrum with energy $E_q = \hbar^2q^2/2m$ are

$$R_q(r) = \frac{2a_{\text{ho}}^{-1/2} \sin(qr - \delta_q)}{r}, \quad (13)$$

where the phase shift δ_q should be determined by the Bethe-Pierels boundary condition $\partial_r(rR_q)/(rR_q)|_{r \rightarrow 0} = -1/a$, and one finds $\tan \delta_q = qa$. At unitarity, $\delta_q = \pi/2$ and thus $R_q(r) = -2a_{\text{ho}}^{-1/2} \cos(qr)/r$. For ideal gas without interaction, $\delta_q = 0$ and thus $R_q(r) = 2a_{\text{ho}}^{-1/2} \sin(qr)/r$. Furthermore, the functions R_q satisfy the orthogonality condition $\int_0^\infty r^2 R_q(r) R_{q'}(r) dr = 2\pi a_{\text{ho}}^{-1} \delta(q - q')$ [38].

The projection of the initial wave function $\psi_0(r)$ on such a basis gives

$$c(q) = \int_0^\infty R_q(r) \psi_0(r) r^2 dr, \quad (14)$$

which provides a useful quantity allowing for the calculation of the density and momentum distributions as a function of time. The behavior of $c(q)$ at large momenta satisfying the condition $q \gg a_{\text{ho}}^{-1}$ is related to the behavior of the wave functions at short distances satisfying the condition $r \ll a_{\text{ho}}$. Substituting the approximated wave function $Aa_{\text{ho}}^{-3/2}(a/r - 1)$ into Eq. (14) and keeping terms up to the first order in a , we find $c(q) \approx 2Aaa_{\text{ho}}^{-2}/q$ if the interaction is turned off and $c(q) = 0$ if the interaction is present during the expansion. In the latter case, the *approximate* initial wave function ψ_0 is orthogonal to R_q as it does not account for the effect of the harmonic trap. A more accurate expression for $c(q)$ is obtained by taking into account that the *exact* initial wave function is only approximately orthogonal to R_q and satisfies the equation $\left(-\frac{\hbar^2}{2m} \frac{d^2}{dr^2} + \frac{1}{2}m\omega_{\text{ho}}^2 r^2 - E\right)(r\psi_0) = 0$. On the other hand the wave function $R_q(r)$ satisfies the equation $\left(-\frac{\hbar^2}{2m} \frac{d^2}{dr^2} - E_q\right)(rR_q) = 0$. Multiplying the first equation by $rR_q(r)$ and the second one by $r\psi_0(r)$, followed by

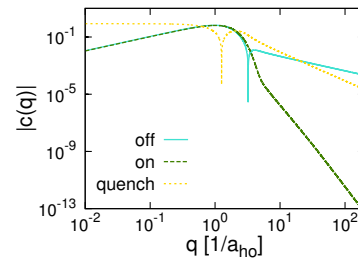


FIG. 2. (Color online) Plot of $|c(q)|$ in the absence of interaction (solid blue line), in the presence of interaction (dashed green line) and after quenching the scattering length to infinity (dotted orange line). The absolute value is added because $c(q)$ changes sign at the dips of the blue and orange lines. The explicit q dependence of $c(q)$ at small and large q is explained in the main text.

an integration with respect to r , and using the fact that *both* wave functions satisfy the Bethe-Pierels boundary condition at $r = 0$, we get

$$c(q) = \frac{\int_0^\infty (m\omega_{\text{ho}}^2 r^2/2)(rR_q)(r\psi_0) dr}{E - \hbar^2q^2/2m}. \quad (15)$$

Note that at the value $q_c = \sqrt{2mE}/\hbar$, the numerator in Eq. (15) vanishes linearly and thus $c(q)$ is well-defined for all values of q . To find the behavior of $c(q)$ at large q , one can again replace $\psi_0(r)$ with the small r approximation. A direct integration gives

$$c(q) \approx -\frac{8Aa}{q^5 a_{\text{ho}}^6 \sqrt{1 + q^2 a^2}}, \quad (16)$$

revealing a much faster decay of $c(q)$ at large q with respect to the case when the interaction is turned off simultaneously with the release of the trap. In particular $c(q) \approx -8Aaa_{\text{ho}}^{-6}/q^5$ if $a_{\text{ho}}^{-1} \ll q \ll a^{-1}$ and $c(q) \approx -8Aaa_{\text{ho}}^{-6}a^{-1}/q^6$ if $q \gg a^{-1}$ [39].

Figure 2 shows the full numerical calculation of $c(q)$ with the exact initial wave function (Eq. (6)). At large momenta (i.e, in the region of $q \gg a_{\text{ho}}^{-1}$), we find $c(q) \propto 1/q$ in the absence of interaction whereas it behaves like $1/q^5$ (for $q \ll a^{-1}$) and $1/q^6$ (for $q \gg a^{-1}$) in the presence of interaction, with the corresponding coefficients in excellent agreement with the above analytic estimate. As already pointed out the momentum distribution preserves its initial form if the interaction is turned off, whereas it dramatically changes during the expansion if the interaction is present. Such a different expansion dynamics is directly connected with the different behaviors exhibited by $c(q)$ at large momenta.

With the help of $c(q)$, the wave function during the expansion can be in fact calculated straightforwardly:

$$\psi(r, \tau) = \int_0^\infty R_q(r) c(q) \exp(-iq^2 a_{\text{ho}}^2 \tau/2) \frac{dq}{2\pi}, \quad (17)$$

and the wave function $\phi(k, \tau)$ in momentum space can be obtained after a direct Fourier transformation.

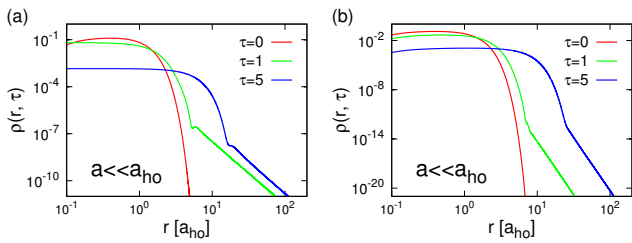


FIG. 3. (Color online) Plot of density distribution (a) in the absence and (b) in the presence of interaction in the expansion. Different colors are the distributions at different expansion time $\tau = 0$ (red) 1 (green), 5 (blue). The linear part of the density distribution $\rho(r, \tau)$ at large r exhibits the $1/r^4$ behavior if the interaction is turned off, whereas it exhibits a $1/r^{12}$ tail followed by a tail of $1/r^{14}$ if the interaction is present.

Let us first consider the case where the interaction is turned off just before the expansion. Since in this case the initial $1/k^4$ large momentum tail is preserved during the expansion, a $1/r^4$ tail at large distance is predicted to develop in the density distribution during the expansion. As shown in Fig. 3(a), a tail of the form $1/r^4$ does actually appear in $\rho(r, \tau)$ at $r/a_{\text{ho}} \gg \tau$, beyond the exponential decay. In terms of $c(k)$, the wave function in momentum space takes the form

$$\phi(k, \tau) = \sqrt{\frac{1}{2\pi}} \frac{a_{\text{ho}}^{1/2}}{k} c(k) e^{-i \frac{k^2 a_{\text{ho}}^2}{2} \tau}. \quad (18)$$

Since $c(k) \approx 2Aa_{\text{ho}}^{-2}/k$ at large k , thus the large momentum distribution $n(k, \tau) = \mathcal{C}_0/k^4$ which, as expected, coincides with the initial one.

If the interaction is not switched off, the expansion dynamics is dramatically different. In Fig. 3(b) we show the density distributions resulting from the direct calculation of Eq. (17). Due to the presence of interaction, the real space density always satisfies $\rho(r = a, \tau) = 0$. Beyond the exponential decay, we find that a tail of the form $\rho(r, \tau) \propto 1/r^{12}$ followed by a tail of the form $\rho(r, \tau) \propto 1/r^{14}$ appears soon after a short expansion time and is preserved afterwards. This can be understood by applying to Eq. (17) the saddle point approximation which is valid at large τ . At the saddle point $q_s = r/(a_{\text{ho}}^2 \tau)$, we find

$$\rho(r, \tau) \approx \frac{1}{2\pi\tau} \frac{|c(q_s)|^2}{r^2 a_{\text{ho}}} = \frac{32A^2 a_{\text{ho}}^7}{\pi} \frac{\tau^9}{r^{12}(1 + r^2 a_{\text{ho}}^2 / (a_{\text{ho}}^4 \tau^2))}. \quad (19)$$

The absence of the $1/r^4$ tail in the density distribution indicates that the $1/k^4$ large momentum tail must disappear after a long enough expansion time. Indeed, as shown in Fig. 4, the large momentum distribution $n(k, \tau) \propto 1/k^4$ decreases and shrinks during the expansion, similarly to the case of the expansion in the presence of unitary interaction (see Fig. 1). Since the momentum distribution reaches the ballistic regime at a different rate

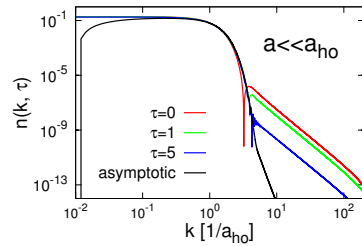


FIG. 4. (Color online) Plot of momentum distribution in the presence of interaction in the expansion. Different colors are the distributions at different expansion time $\tau = 0$ (red) 1 (green), 5 (blue) and the asymptotic momentum distribution (black). The linear part of the momentum distribution at large k exhibits a tail of $1/k^4$ whereas the asymptotic momentum distribution exhibits a $1/k^{12}$ tail followed by a $1/k^{14}$ tail at large k .

for different momenta, strong interference oscillations appear in the intermediate momentum regime connecting the low and large momentum sectors. A careful analysis shows that the average of these oscillations results in a $1/k^{12}$ behavior with the increase of time. Therefore, when the ballistic relation is satisfied, the momentum distribution should exhibit a $1/k^{12}$ tail followed by a $1/k^{14}$ tail at $\tau \rightarrow \infty$, consistently with the large r behavior of the density distribution (see Eq. (19)).

To investigate the time-dependence of the $1/k^4$ large momentum tail at large but finite τ , it is important to calculate the evolution of the wave function at small r . In this case only the small momentum behavior of $c(q)$ is important for the integration in Eq. (17) where $c(q) \approx -A\sqrt{2\pi}a_{\text{ho}}q$ (see Fig. 2). Thus, the wave function is $\psi(r, \tau) \approx Aa_{\text{ho}}^{-3/2} e^{i(r-a)^2/2\tau} (a/r - 1)/(i\tau)^{3/2}$ at small r . The exponential phase factor can be dropped at large time and the momentum distribution behaves like $n(k, \tau) \approx n_0(k)/\tau^3$ at large k . In conclusion the contact decreases as $\mathcal{C}(t) = \mathcal{C}_0/t^3$ for $t \gg 1/\omega_{\text{ho}}$ which agrees with the numerical calculation of $n(k, \tau)$ shown in Fig. 4. The time dependence of the decay is the same as in the case of the weakly interacting Bose gas discussed in the first part of the paper, thereby providing a justification of the adiabatic ansatz employed to derive the $1/t^3$ decay law.

C. Quench dynamics

In the last part of the work we consider the time evolution of the contact after a quench of the scattering length from a small value to $a = \infty$ just before the expansion. This problem, already investigated both experimentally[22, 25] and theoretically[23, 24] in the presence of a harmonic trap, will be considered here by switching off the trap simultaneously with the quench of the scattering length.

At unitarity, the continuum eigenstates are $R_q(r) =$

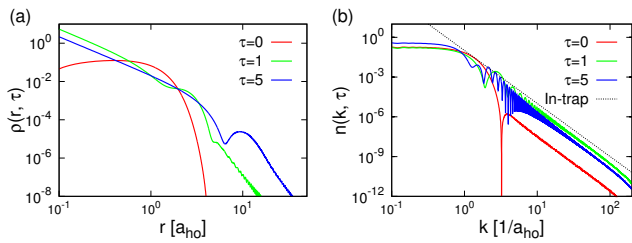


FIG. 5. (Color online) Plot of (a) density and (b) momentum distributions in the expansion with the scattering quenched to $a = \infty$ at $\tau = +0$. Different colors are the distributions at different expansion time $\tau = 0$ (red), 1 (green), 5 (blue). The black dotted line indicates the position of the large momentum tail for the in-trap equilibrium system with unitary interaction. The linear part of the density distribution at large r exhibits a tail of $1/r^6$ at large times. The linear part of the momentum distribution at large k exhibits a tail of $1/k^4$ which first increases at short times and then decreases at larger expansion times.

$-2a_{\text{ho}}^{-1/2} \cos(qr)/r$. Using the approximated form of the initial wave function $\psi_0(r) \approx Aa_{\text{ho}}^{-3/2}(a_0/r - 1)$ at small r , where a_0 is the scattering length before the quench, we get $c(q) \approx -2A/(q^2 a_{\text{ho}}^2)$ at large q (see Fig. 2). Applying the saddle point approximation to Eq. (17) at the saddle point $q_s = r/(a_{\text{ho}}^2 \tau)$, one then finds

$$\rho(r, \tau) \approx \frac{1}{2\pi\tau} \frac{|c(q_s)|^2}{r^2 a_{\text{ho}}} = \frac{2A^2 a_{\text{ho}}^3}{\pi} \frac{\tau^3}{r^6}. \quad (20)$$

Using the ballistic relation (Eq. (1)), we find that the asymptotic momentum distribution behaves like $1/k^6$. Consequently, the $1/k^4$ tail of the momentum distribution should evolve into $1/k^6$ after long expansion time. Figure 5 shows the time-dependent evolution of the density and momentum distributions in the expansion after quenching the scattering length from $a_0 = 0.05a_{\text{ho}}$ to $a = \infty$. A tail of the form $1/r^6$ is developed in the density distribution, in good agreement with the above analytical calculation. The momentum distribution can be separated into two stages. At shorter times, the two-body correlations increase due to the quench and the $1/k^4$ tail increases and quickly reaches the in-trap equilibrium value, as investigated in Ref. [23]. At longer times, the expansion dynamics dominates and the contact decreases, in agreement with our previous results for the unitary interaction. Since the rate of the evolution is slow, a new $1/k^6$ tail is expected to appear after a long expansion time.

IV. CONCLUSION

In this paper we have investigated the time-dependence of the density and momentum distribution of various expanding physical systems after the release from a harmonic trap, with special focus on the behavior of the

contact parameter. We have explicitly shown that the momentum distribution changes dramatically if the interaction is present during the expansion and the large momentum tail decreases and eventually disappears for large times. On the other hand, differently from the case when the interaction is switched off before the expansion, the density distribution, which is the observable quantity in the time-of-flight experiments, does not exhibit any $1/r^4$ behavior, even at intermediate times where the $1/k^4$ tail in the momentum distribution is still visible. So far, our investigations have been devoted to isotropically trapped systems. The presence of anisotropy in the trapping potential is not expected to introduce major differences in the large k behavior of the momentum distribution of the expanding gas, although its role might deserve further theoretical investigation.

On the basis of our results we conclude that the $1/r^4$ density tail, observed after the release of an anisotropic trap in the recent experiment by R. Chang, *et. al* carried out on a weakly interacting Bose gas of metastable ^4He atoms [26], is still elusive and remains an open problem to understand.

Note added.— In the preparation of the manuscript, we noticed a preprint by S. E. Gharashi and D. Blume[40] on the evolution of the contact for a smoothly released one dimensional harmonic trap.

ACKNOWLEDGMENTS

We would like to thank David Clemént and Alain Aspect for stimulating our interest in the problem of the contact during the expansion and for informing us about their recent experiment on the expansion of metastable ^4He atoms. Useful correspondence and discussions with Shina Tan, Stefano Giorgini and Christophe Salomon are acknowledged. C. Qu thanks Yangqian Yan for helpful discussions. This work was supported by the QUIC grant of the Horizon2020 FET program and by Provincia Autonoma di Trento.

Appendix A: One-body density matrix

Using the scaling law (Eq. (2)), an exact relationship can be obtained also for the time dependence of the one-body density matrix,

$$\rho^{(1)}(\mathbf{r}, \mathbf{r}', t) = \frac{1}{b^3} e^{-i\frac{m}{2\hbar} \frac{b}{b} (\mathbf{r}^2 - \mathbf{r}'^2)} \rho_0^{(1)} \left(\frac{\mathbf{r}}{b}, \frac{\mathbf{r}'}{b} \right). \quad (\text{A1})$$

Introducing the sum and difference of these two position vectors, $\mathbf{R} = (\mathbf{r} + \mathbf{r}')/2$ and $\mathbf{s} = (\mathbf{r} - \mathbf{r}')$, and taking the Fourier transformation, one then obtains the exact result

$$n(\mathbf{k}, t) = \frac{1}{(2\pi)^3} \frac{1}{b^3} \int d\mathbf{R} d\mathbf{s} \left[e^{-i\mathbf{s} \cdot (\mathbf{k} - \frac{m\mathbf{b}}{\hbar b} \mathbf{R})} \rho_0^{(1)} \left(\frac{\mathbf{R}}{b}, \frac{\mathbf{s}}{b} \right) \right] \quad (\text{A2})$$

for the momentum distribution at time t , in terms of the initial value of the one-body density matrix.

To calculate the asymptotic momentum distribution $n_{\text{asym}} = \lim_{t \rightarrow \infty} n(\mathbf{k}, t)$ it is convenient to introduce the rescaled variable $\tilde{R} = R/b(t)$. At large times, where $b(t) \rightarrow \omega_{\text{ho}} t$, one then easily finds the result

$$\begin{aligned} & \lim_{t \rightarrow \infty} n(\mathbf{k}, t) \\ &= \left(\frac{\hbar}{m\omega_{\text{ho}}} \right)^3 \int d\tilde{\mathbf{R}} \delta(\tilde{\mathbf{R}} - \frac{\hbar}{m\omega_{\text{ho}}} \mathbf{k}) \rho_0^{(1)}(\tilde{\mathbf{R}}, 0) \\ &= \left(\frac{\hbar}{m\omega_{\text{ho}}} \right)^3 \rho_0 \left(\tilde{\mathbf{R}} = \frac{\hbar}{m\omega_{\text{ho}}} \mathbf{k} \right), \end{aligned} \quad (\text{A3})$$

which coincides with the result (Eq. (4)) derived in Sec. II employing the ballistic relation.

The time-dependence of the contact at finite expansion times can be also obtained by calculating the asymptotic behavior of Eq. (A2) at large k . For large momenta satisfying $k \gg \frac{mb}{\hbar} R_0$ which implies $ka_{\text{ho}} \gg R_0/a_{\text{ho}}$, with R_0 the initial size of the trapped gas, the variable \mathbf{R} can be ignored in the exponential factor of Eq. (A2) and the momentum distribution approaches the scaling behavior

$$n(\mathbf{k}, t) \rightarrow b^3(t) n(\mathbf{k}b(t)). \quad (\text{A4})$$

As a consequence, the contact takes the form

$$\mathcal{C}(t) = \frac{C_0}{b(t)}, \quad (\text{A5})$$

which coincides with the result obtained using the adiabatic ansatz for the unitary Fermi gas.

-
- [1] S. Tan, *Ann. Phys.* **323**, 2952 (2008); **323**, 2971 (2008); **323**, 2987 (2008).
- [2] M. Olshanii and V. Dunjko, *Phys. Rev. Lett.* **91**, 090401 (2003).
- [3] E. Braaten and L. Platter, *Phys. Rev. Lett.* **100**, 205301 (2008).
- [4] S. Zhang and A. J. Leggett, *Phys. Rev. A* **79**, 023601 (2009).
- [5] F. Werner, L. Tarruell, and Y. Castin, *Eur. Phys. J. B* **68**, 401 (2009).
- [6] E. D. Kuhnle, H. Hu, X.-J. Liu, P. Dyke, M. Mark, P. D. Drummond, P. Hannaford, and C. J. Vale, *Phys. Rev. Lett.* **105**, 070402 (2010).
- [7] M. Barth and W. Zwerger, *Ann. Phys.* **326**, 2544 (2011).
- [8] R. J. Wild, P. Makotyn, J. M. Pino, E. A. Cornell, and D. S. Jin, *Phys. Rev. Lett.* **108**, 145305 (2012).
- [9] K. Xu, Y. Liu, D. E. Miller, J. K. Chin, W. Setiawan, and W. Ketterle, *Phys. Rev. Lett.* **96**, 180405 (2006).
- [10] S. Utsunomiya, L. Tian, G. Roumpos, C. W. Lai, N. Kumada, T. Fujisawa, M. Kuwata-Gonokami, A. Löffler, S. Höfling, A. Forchel, and Y. Yamamoto, *Nature Physics* **4**, 700 (2008).
- [11] J. T. Stewart, J. P. Gaebler, T. E. Drake, and D. S. Jin, *Phys. Rev. Lett.* **104**, 235301 (2010).
- [12] Y. Sagi, T. E. Drake, R. Paudel, and D. S. Jin, *Phys. Rev. Lett.* **109**, 220402 (2012).
- [13] R. Haussmann, *Phys. Rev. B* **49**, 12975 (1994).
- [14] F. Palestini, A. Perali, P. Pieri, and G. C. Strinati, *Phys. Rev. A* **82**, 021605(R) (2010).
- [15] E. D. Kuhnle, S. Hoinka, P. Dyke, H. Hu, P. Hannaford, and C. J. Vale, *Phys. Rev. Lett.* **106**, 170402 (2011).
- [16] J. E. Drut, T. A. Lähde, and T. Ten, *Phys. Rev. Lett.* **106**, 205302 (2011).
- [17] H. Hu, X.-J. Liu and P. D. Drummond, *New. J. Phys.* **13**, 035007 (2011).
- [18] Y. Yan and D. Blume *Phys. Rev. A* **88**, 023616 (2013).
- [19] S. Hoinka, M. Lingham, K. Fenech, H. Hu, C. J. Vale, J. E. Drut, and S. Gandolfi, *Phys. Rev. Lett.* **110**, 055305 (2013).
- [20] D. H. Smith, E. Braaten, D. Kang, and L. Platter, *Phys. Rev. Lett.* **112**, 110402 (2014).
- [21] S. Laurent, X. Leyronas, and F. Chevy, *Phys. Rev. Lett.* **113**, 220601 (2014).
- [22] P. Makotyn, C. E. Klauss, D. L. Goldberger, E. A. Cornell, and D. S. Jin, *Nat. Phys.* **10**, 116 (2014).
- [23] A. G. Sykes, J. P. Corson, J. P. D’Incao, A. P. Koller, C. H. Greene, A. M. Rey, K. R. A. Hazzard, and J. L. Bohn, *Phys. Rev. A* **89**, 021601(R) (2014).
- [24] J. P. Corson and J. L. Bohn, *Phys. Rev. A* **94**, 023604 (2016).
- [25] R. J. Fletcher, R. Lopes, J. Man, N. Navon, R. P. Smith, M. W. Zwierlein, and Z. Hadzibabic, [arXiv:1608.04377](https://arxiv.org/abs/1608.04377)
- [26] R. Chang, Q. Bouton, H. Cayla, C. Qu, A. Aspect, C. I. Westbrook, and D. Clément, [arXiv:1608.04693](https://arxiv.org/abs/1608.04693)
- [27] L. P. Pitaevskii and S. Stringari, *Bose-Einstein Condensation and Superfluidity*, (Oxford University Press, New York, 2016).
- [28] Yu. Kagan, E. L. Surkov, and G.V. Shlyapnikov, *Phys. Rev. A* **54**, 1753 (1996)(R).
- [29] Y. Castin and R. Dum, *Phys. Rev. Lett.* **77**, 5315 (1996).
- [30] F. Dalfvo, C. Minniti, S. Stringari, L. P. Pitaevskii, *Phys. Lett. A* **227**, 259 (1997).
- [31] Y. Castin, *C. R. Physique* **5**, 407 (2004).
- [32] C. Chin, R. Grimm, P. Julienne, and E. Tiesinga, *Rev. Mod. Phys.* **82**, 1225 (2010).
- [33] T. Busch, B.-G. Englert, K. Rzazewski, and M. Wilkens, *Foundations of Physics*, **28**, 549 (1998).
- [34] $F(z) = z - 2z^3/3 + 4z^5/15 - \dots$ for $|z| \rightarrow 0$ and $F(z) = 1/(2z) + 1/(4z^3) + 1/(8z^5) + \dots$ for $\arg(z) < \pi/4$ and $|z| \rightarrow \infty$ (see, for example, J. H. McCabe, *Mathematics of computation*, **28**, 811 (1974)).
- [35] This condition requires larger and larger values of k as τ increases.
- [36] F. W. J. Olver, D. W. Lozier, R. F. Boisvert, and C. W. Clark, *NIST Handbook of Mathematical Functions* (Cambridge University Press, New York, 2010).
- [37] We consider here the second energy level of Eq. (7) to avoid the use of the first energy level of the pseudopotential interaction which corresponds to a bound state for $a > 0$ in the absence of the harmonic trap.
- [38] L. D. Landau and E. M. Lifshitz, *Quantum Mechanics: non-relativistic theory*, 3rd ed. (Butterworth Heinemann,

1977).

- [39] It is worth to note that the regime $c(q) \propto 1/q^6$ does not exist in the hard sphere model where the range of interaction $r_0 = a$, because the whole theory is valid at the condition $qr_0 \ll 1$. However, this regime can be reached if $a \gg r_0$.
- [40] S. E. Gharashi and D. Blume, [arXiv:1608.05708](https://arxiv.org/abs/1608.05708)